Femtosecond Spectroscopy of Optical Excitations in Single-Walled Carbon Nanotubes: Evidence for Exciton-Exciton Annihilation

Ying-Zhong Ma,[1] Leonas Valkunas,[1,2] Susan L. Dexheimer,[1,*] Sergei M. Bachilo,[3] and Graham R. Fleming[1]

[1]*Department of Chemistry, University of California, Berkeley, and Physical Biosciences Division, Lawrence Berkeley National Laboratory, Berkeley, California 94720-1460, USA*

[2]*Institute of Physics, Savanoriu Avenue 231, 02300 Vilnius, Lithuania, and Theoretical Physics Department, Faculty of Physics of Vilnius University, Sauletekio Avenue 9, building 3, 10222 Vilnius, Lithuania*

[3]*Department of Chemistry and Center for Biological and Environmental Nanotechnology, Rice University, 6100 Main Street, Houston, Texas 77005, USA*

(Received 28 October 2004; published 21 April 2005)

Frequency-resolved femtosecond transient absorption spectra and kinetics measured by optical excitation of the second and first electronic transitions of the (8, 3) single-walled carbon nanotube species reveal a unique mutual response between these transitions. Based on the analysis of the spectra, kinetics, and their distinct amplitude dependence on the pump intensity observed at these transitions, we conclude that these observations originate from both the excitonic origin of the spectrum and nonlinear exciton annihilation.

DOI: 10.1103/PhysRevLett.94.157402 PACS numbers: 78.47.+p, 71.35.-y, 78.67.Ch

Single-walled carbon nanotubes (SWNT) are elongated (quasi-1D) structures belonging to the fullerene family with unique physical properties [1,2]. Depending on its diameter and chirality, a SWNT can exhibit either metallic or semiconducting characteristics [2,3]. The strong dependence of physical properties on the structure of SWNTs and the anticipation of attracting device applications [4] has led to many studies of the various features of these systems.

Femtosecond optical spectroscopy has been applied to probe charge carrier or exciton creation, their relaxation, and other relevant physical mechanisms in many nanometer-scale materials [5,6]. Several femtosecond spectroscopic studies of SWNTs have also been reported, performed using either transient absorption [7–12] or fluorescence up-conversion [10,13] techniques. The results obtained for the semiconducting nanotubes were attributed either to optical transitions between van Hove singularities of the valence and conduction bands of (quasi)-1D systems according to the one-electron scheme with a subsequent relaxation of charged carriers [7,8,12] or to excitonic transitions [9,10] according to theoretical calculations which include multiparticle interactions [14,15]. In addition to the debate on the fundamental physics of this material, the time constants reported from different groups also vary remarkably, reflecting perhaps the variation of excitation and/or detection wavelength, pulse duration, excitation intensity, and sample state (individual tube enriched aqueous solutions versus solid films made of bundles and/or ropes of SWNT). Detection of ultrafast spectroscopic and dynamic information for selected tube species is highly desirable, and should help to remove the existing inconsistencies.

In this Letter, we present experimental data collected for an *individual* semiconducting nanotube species, (8, 3), using the femtosecond transient absorption technique on an individual nanotube enriched SWNT preparation suspended in an aqueous solution of sodium dodecyl sulfate micelles [16]. The observed spectroscopic and dynamic responses are elucidated with an exciton (the electron-hole pair coupled by Coulomb interaction) model presented in Fig. 1, emphasizing exciton-exciton annihilation as a predominant mechanism responsible for their initial relaxation.

Experiments were carried out with a SWNT material produced by a high-pressure CO (HiPco)–type generator, and the procedure described in [16] was used to prepare a sample rich in individual nanotubes in a surfactant-water system (SDS in H_2O). The optical density of the sample was kept below 0.2 at the pump wavelength in order to avoid an inhomogeneous distribution of excitations in the excited volume and reabsorption of the excited species. Sub-100 fs broadband transient absorption (TA) experiments were performed using a 250 kHz regenerative amplified Ti:sapphire system [10], and a spectrograph with a Peltier-cooled charge coupled device (CCD) camera served as the detection spectrometer. The details of the experimental setup will be published elsewhere.

Figures 2(a) and 2(b) show the TA spectra recorded in the visible and near infrared (NIR) regions at delay times (t_p) of 50 fs and 1 ps, respectively. The pump pulses (λ_{pu}) are centered at 660 and 953 nm, respectively, which are electronically resonant with transitions to the second, $E_2(k)$, and the first, $E_1(k)$, exciton bands (according to our definitions given in Fig. 1) of the (8, 3) nanotube structure [17]. Excitation to the $E_2(k)$ exciton state with $\lambda_{pu} = 660$ nm leads to a broad induced transmission (IT) band around 660 nm attributed to the removal of population from the ground state of the (8, 3) SWNT as well as of other nanotubes, including (7, 5), (7, 6), and (9, 5), because

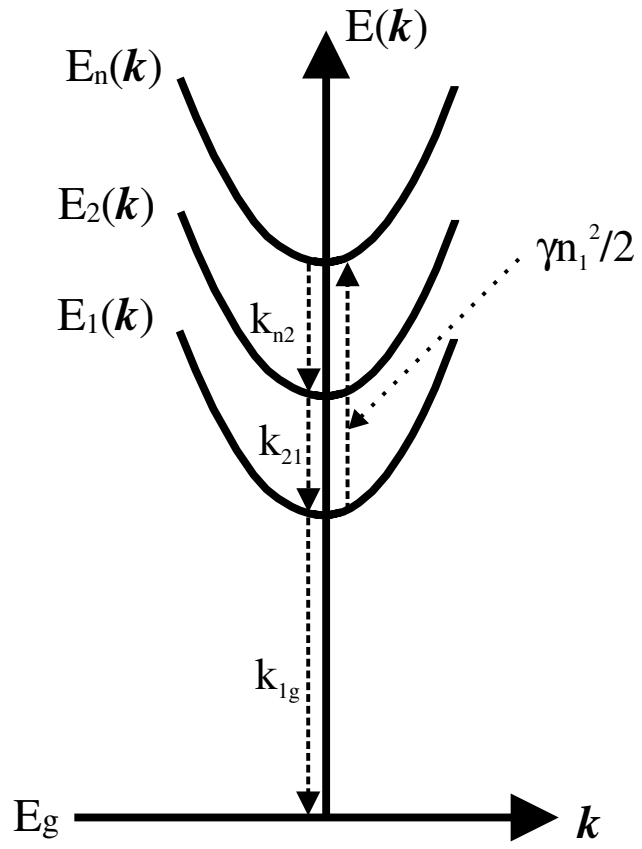

FIG. 1. Schematic model describing the exciton dynamics in a semiconducting SWNT. E_g and $E_i(k)$ represent the ground state and the ith exciton band, respectively, k is the exciton center-of-mass momentum, and arrows depict the transitions between the exciton bands caused by relaxation. k_{ij} describes the relaxation rate from the ith exciton state to the jth exciton state, and $\gamma n_1^2/2$ is the rate of populating a higher exciton state as the result of exciton-exciton annihilation.

of their closely located excitonic transitions [10,17]. At the same time, a major IT band peaked at 954 nm is also observed, resulting from ground state depletion and population of the $E_1(k)$ state following relaxation from $E_2(k)$ [10,17]. These IT bands further show a good match with the resolvable peaks in the linear absorption spectrum (Fig. 2, solid lines). Additional IT bands appear at 731 and 1026 nm as well as structureless, induced absorption signals over the rest of the detected spectral region. The origins of these signals and their dynamic behavior will be discussed elsewhere.

In comparison, resonant excitation into the $E_1(k)$ exciton band of the (8, 3) tube species with $\lambda_{pu} = 953$ nm results in two strongly overlapped IT bands at $t_p < 1$ ps, which subsequently evolve into two separate bands peaked at 954 and 975 nm, respectively [Fig. 2(b)]. These bands correspond to the transitions of the (8, 3) and (6, 5) nanotubes [17], concurrently excited because of their similar $E_1(k)$ energies. Remarkably, excitation of the $E_1(k)$ band also leads to the formation of a weak IT band peaking at 664 nm, which matches precisely the frequency of the corresponding $E_2(k)$ transition of the (8, 3) tube. In comparison to the IT band observed with direct $E_2(k)$ excitation [Fig. 2(a), filled circles], this weak IT band appears significantly narrowed, probably due to variation of the contributing tube types in accordance with the change of the pump wavelength.

Though optical excitation into the $E_1(k)$ exciton band causes bleaching of both transitions into the $E_1(k)$ and $E_2(k)$ exciton bands of the (8, 3) tube species, these TA signals display strikingly different excitation intensity dependences. A set of transients were measured at 660 and 953 nm under different intensities of pump pulses centered at 953 nm, and their maximum amplitudes are plotted in Fig. 3 versus the pump intensity. It is evident from Fig. 3 that the amplitude of the bleaching signal for the transition into the $E_2(k)$ exciton band scales linearly with the excitation intensity, while that detected for the transition into the $E_1(k)$ exciton band shows saturation behavior.

The strikingly different intensity dependence shown in Fig. 3 can be understood in terms of the exciton model presented in Fig. 1. Besides the mutual bleaching of both exciton states independent of the excitation wavelength (see Fig. 2), the kinetics for both exciton transitions are modulated by population relaxation. At high excitation intensities, nonlinear exciton-exciton annihilation takes place [10]. This process describes the mutual interaction of excitons with a rate of $\frac{1}{2}\gamma n_1^2(t)$ [18,19], where $n_1(t)$ is the

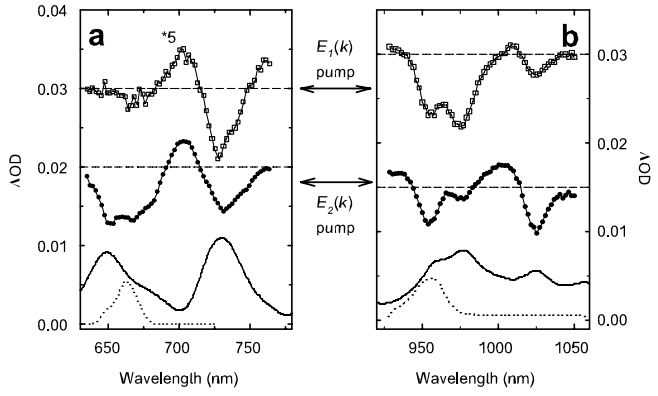

FIG. 2. Transient absorption spectra measured in the visible (a) and NIR (b) regions upon excitation at 660 (filled circles) and 953 nm (open squares). The spectra are recorded at delay times of 50 fs and 1 ps, respectively, with a pump fluence of $\sim 10^{14}$ photons/pulse cm^2. Those excitation conditions correspond to transitions into the $E_2(k)$ and $E_1(k)$ exciton bands as indicated in the scheme shown in Fig. 1, respectively. The solid line is the linear absorption spectrum in the relevant region (scaled for ease of visualization), and the dotted lines are the spectra of the pump pulses. The transient absorption spectra are vertically offset for clarity, and the thin dashed lines are the baselines ($\Delta OD = 0$).

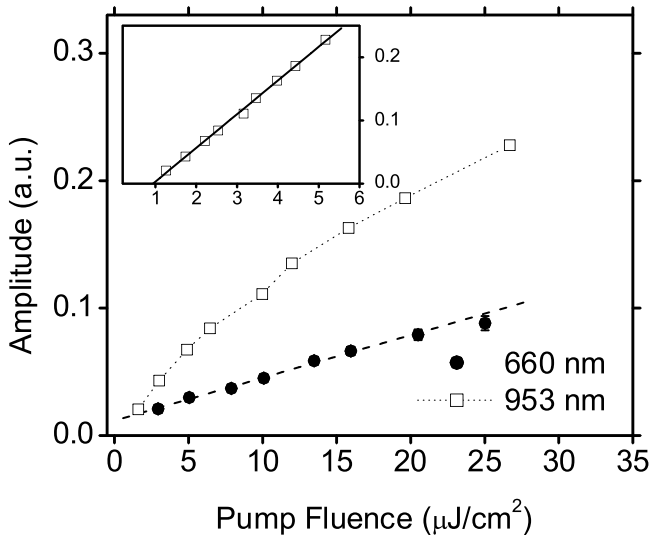

FIG. 3. Plot of the maximum amplitude of the transient absorption kinetics probed at 660 nm (filled circles) and 953 nm (open squares) versus the intensity of the pump pulses at 953 nm. The dashed line is the linear fit of the data obtained by probing at 660 nm, and the dotted line is drawn to guide the eye for the data obtained by probing at 953 nm. The inset shows the same data measured at 953 nm, but plotted on the scale of the square root of pump intensity. The solid line represents the linear fit.

$E_1(k)$ exciton population and γ is the value determining the nonlinear annihilation rate. As a result, both excitons disappear with the simultaneous induction of population into higher excited states located in the vicinity of the doubly $E_1(k)$ exciton state, which is schematically indicated as $E_n(k)$. This band may be related to the electron-hole continuum according to *ab initio* calculations [14,15]. Kinetic equations describing the exciton relaxation are easily deduced from the scheme shown in Fig. 1. The rate populating the doubly excited state is half of the annihilation rate, i.e., $\frac{1}{2}\gamma n_1^2$ as indicated in Fig. 1. Since the relaxation rates k_{n2} and k_{21} between corresponding exciton bands are very fast [10], the population of the $E_2(k)$ exciton state, $n_2(t)$, caused by the exciton-exciton annihilation has to follow the pumping rate of the higher excited states, i.e.,

$$n_2(t) \cong \frac{1}{2k_{21}}\gamma n_1^2(t), \tag{1}$$

while the population of the lowest exciton state $E_1(k)$ is determined by the following kinetic equation:

$$\frac{dn_1(t)}{dt} = G(t) - \frac{1}{2}\gamma n_1^2(t) - k_{1g}n_1(t), \tag{2}$$

where $G(t)$ is the exciton generation rate and k_{1g} is the rate of exciton relaxation to the ground state (i.e., electron-hole recombination). In the case of high intensity excitation when the nonlinear annihilation process dominates linear relaxation, the quasistationary solution of Eq. (2) will relate the population amplitudes $n_1(0)$ and $n_2(0)$ with the amplitude of the excitation pumping $G(t_{\max})$, thus giving

$$n_1^2(0) \approx \frac{2}{\gamma}G(t_{\max}), \tag{3}$$

which, by substituting into Eq. (1), gives the following relationship:

$$n_2(0) \approx \frac{1}{k_{21}}G(t_{\max}). \tag{4}$$

According to Eq. (4), the TA signal probed at the $E_2(k)$ transition should be linearly dependent on the intensity of the excitation pulses resonant with the $E_1(k)$ transition, while saturation behavior is expected for the TA signal probed at the $E_1(k)$ transition [Eq. (3)].

The actual population created in the $E_2(k)$ exciton state via annihilation of the $E_1(k)$ excitons is strongly supported by the excellent match between the squared profile recorded at 953 nm and the kinetics obtained at 660 nm as shown in Fig. 4(a), both measured upon excitation of $E_1(k)$. This match is in accord with Eq. (1), which holds if the exciton-exciton annihilation is the dominant channel for exciton relaxation during an extended time scale of at least 20 ps, thus resulting in population of the $E_2(k)$ exciton state. To the best of our knowledge, this match provides the first example of a higher-lying electronic state being populated via exciton annihilation on such an extended time scale [20].

Closer examination of the kinetics measured at 953 nm under various pump intensities reveals negligible dependence in terms of their decay behavior. As an example, Fig. 4(b) shows the data collected at the lowest and the highest pump intensity, which differ by 17 times. This independence can be understood by considering the formal

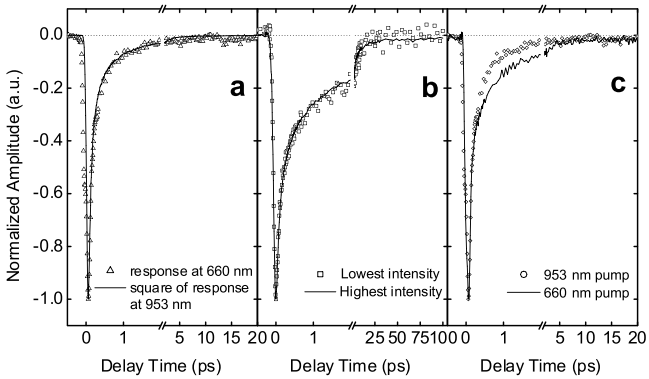

FIG. 4. (a) Comparison of the squared profile at 953 nm (solid line) and the kinetics at 660 nm; both data are recorded with the $E_1(k)$ excitation. (b) Kinetics probed at 953 nm under the lowest (open squares) and highest (solid line) pump intensities at 953 nm. (c) Kinetics probed at 660 nm upon resonant excitation of the $E_1(k)$ (open squares) and $E_2(k)$ (solid line) exciton bands of the (8, 3) nanotubes. All kinetics shown in (a)–(c) are normalized at the signal maxima.

solution of Eq. (2):

$$n_1(t) = \frac{n_1(0)e^{-k_{1g}t}}{1 + n_1(0)\gamma(1 - e^{-k_{1g}t})/2k_{1g}}. \quad (5)$$

For time scales short in comparison with the inverse of the linear relaxation rate and for reasonably high excitation intensities, the unity in the denominator of Eq. (5) can be discarded. This results in a simplified form of Eq. (5), which describes pump intensity independent kinetics of the population. Reasonable fits of the experimental data can be obtained with this simplified form of Eq. (5) in the presence of an additional exponential decay term, suggesting some contribution from other tube species on a longer time scale (> 3 ps). Nevertheless, the fits strongly support our conclusion that very fast exciton-exciton annihilation dominates the initial decay.

Additional important support for the formation of the $E_2(k)$ exciton state via exciton annihilation comes from the nearly identical transients probed at 660 nm following the excitation of the $E_1(k)$ and $E_2(k)$ transitions as shown in Fig. 4(c). Both the decays begin with a dominant, pulse-width limited decay, which, in view of its match with the fluorescence rise kinetics probed at $E_1(k)$ [10], can be confidently attributed to the relaxation between exciton states. This pulse-width-limited decay component is followed by a much slower decay with overall amplitude amounting to 20%, which fully recovers at a delay time of 20 ps. A subtle difference between these profiles at delay times >300 fs is also noticed, resulting from either unwanted tube species or a secondary correlation with the $E_1(k)$ state. This correlation can be understood by considering that excitonic states share a common ''ground state.'' The density of electronic states consists of some continuum portions in addition to the van Hove singularities [2,14], which overlap between different valence and conduction band states. Consequently, the exciton of a given transition will be made up of the electron-hole pairs not only from the respective valence and conduction band states but also from other states, resulting in mixing of the characteristics associated with resonance excitonic states [21]. A quantitative characterization of this secondary correlation will be made in combination with *ab initio* calculations of the electronic structure of selected semiconducting nanotubes, and the results will be reported elsewhere.

In conclusion, the application of the frequency-resolved femtosecond TA technique on a micelle dispersed SWNT preparation reveals a unique spectroscopic response of the second exciton state of a specific tube type (8, 3) to the optical excitation of its lowest one. Analysis of the temporal, spectral, and intensity profiles of our signals enable us to unambiguously identify the predominant dynamical process as a remarkable manifestation of exciton-exciton annihilation. In typical semiconductor quantum dots and wires, annihilation occurs on a time scale that is at least 1 order of magnitude longer than in SWNT [22]. This extremely rapid annihilation in SWNT and its persistence to an extended time scale imply that very extensive delocalization is an intrinsic property of excitons in semiconducting SWNT. Our observations further provide experimental evidence for the excitonic nature of the elementary excitation in individual semiconducting nanotubes.

The work at Berkeley was supported by the NSF. S. M. B acknowledges support under NSF CHE-031427 and EEC-0118007. L. V. thanks the Fulbright Foundation for financial support. We thank J. Stenger, S. G. Louie, and C. D. Spataru for helpful discussion, and R. E. Smalley for providing the HiPco SWNT materials.

*Permanent address: Department of Physics, Washington State University, Pullman, WA 99164-2814, USA.

[1] M. S. Dresselhaus, G. Dresselhaus, and P. C. Eklund, *Science of Fullerences and Carbon Nanotubes* (Academic Press, San Diego, 1996).
[2] S. Saito, G. Dresselhaus, and M. S. Dresselhaus, *Physical Properties of Carbon Nanotubes* (Imperial College Press, London, 1998).
[3] T. W. Odom *et al.*, J. Phys. Chem. B **104**, 2794 (2000).
[4] R. H. Baughman, A. A. Zakhidov, and W. A. de Heer, Science **297**, 787 (2002).
[5] V. I. Klimov, J. Phys. Chem. B **104**, 6112 (2000).
[6] A. J. Nozik, Annu. Rev. Phys. Chem. **52**, 193 (2001).
[7] J.-S. Lauret *et al.*, Phys. Rev. Lett. **90**, 057404 (2003).
[8] G. N. Ostojic *et al.*, Phys. Rev. Lett. **92**, 117402 (2004).
[9] O. J. Korovyanko *et al.*, Phys. Rev. Lett. **92**, 017403 (2004).
[10] Y.-Z. Ma *et al.*, J. Chem. Phys. **120**, 3368 (2004).
[11] A. Hagen *et al.*, Appl. Phys. A **78**, 1137 (2004).
[12] L. Huang, H. N. Pedrosa, and T. D. Krauss, Phys. Rev. Lett. **93**, 017403 (2004).
[13] F. Wang *et al.*, Phys. Rev. Lett. **92**, 177401 (2004).
[14] C. D. Spataru *et al.*, Phys. Rev. Lett. **92**, 077402 (2004).
[15] C. D. Spataru *et al.*, Appl. Phys. A **78**, 1129 (2004).
[16] M. J. O'Connell *et al.*, Science **297**, 593 (2002).
[17] S. M. Bachilo *et al.*, Science **298**, 2361 (2002).
[18] L. Valkunas, G. Trinkunas, and V. Liuolia, in *Resonance Energy Transfer*, edited by D. L. Andrews and A. A. Demidov (John Wiley & Sons, Chichester, 1999), p. 244.
[19] H. van Amerongen, L. Valkunas, and R. van Grondelle, *Photosynthetic Excitons* (World Scientific, Singapore, 2000), p. 479.
[20] This type of the intensity dependence is expected when the absorption from the $E_1(k)$ exciton band compensates the ground state bleaching in the vicinity of the transition into the $E_2(k)$ exciton band.
[21] V. Perebeinos, J. Tersoff, and P. Avouris, Phys. Rev. Lett. **92**, 257402 (2004).
[22] H. Htoon, J. A. Hollingsworth, R. Dickerson, and V. I. Klimov, Phys. Rev. Lett. **91**, 227401 (2003).